The effect of leaf shape on the interception of solar radiation

C.B.S. Teh*

Department of Land Management, Universiti Putra Malaysia, 43400 UPM Serdang, Selangor, Malaysia

Abstract

One of the properties of canopy architecture is leaf shape, and its effect on solar radiation interception by a plant is little understood and studied. Consequently, this study was to evaluate the effect of six leaf shapes on both direct and diffuse solar radiation interception using a detailed 3-D solar radiation model. Six hypothetical plant prototypes were computer-generated so that each prototype was equal to each other in all aspects; only the leaf shape for each prototype was varied. The leaf shapes selected were round (RD), square (SQ), triangle (TR), inverted triangle (ITR), ellipse (EL) and lobe (LB). Computer simulations revealed that leaf shape did have an effect on direct and diffuse solar radiation interception. However, its effect was to a rather small extent of not more than 11% increase in solar radiation interception. The mean hourly interception of solar radiation by the prototypes decreased in the following manner: (ITR ≈ EL) > (RD ≈ SQ ≈ TR ≈ LB). Although leaf lobbing is often hypothesised to produce deeper sunflecks within the canopy, this study however revealed that leaf lobbing *per se* had no effect on solar radiation interception. All properties being equal, solar radiation interception could be increased by having leaf shapes that are: 1) long and narrow, 2) broader at the apex than at the basal, and 3) supported by leaf petioles. These three conditions increase solar radiation interception by causing the canopy to be spread out more uniformly in the aerial space; this, in turn, means less leaf clustering and self-shading. However, the effect of leaf shape on solar radiation interception decreases for near or full canopy cover because at this stage, the canopy is already intercepting solar radiation at near maximum capacity. Leaf shape also did not affect the diurnal variation of direct and diffuse solar radiation interception. This study may help to better select crop varieties having the "proper leaf form" for optimum plant production, as well as to better understand plant adaptation mechanisms in response to environmental stresses.

Keywords: leaf shape; solar radiation; Beer's law; canopy architecture

* Tel: +60-3-89466976; Fax: +60-3-89434419; Email: chris@agri.upm.edu.my

1. Introduction

Canopy architecture strongly affects a plant's capability to intercept solar radiation. This is because canopy architecture is the geometrical property and spatial arrangement of the plant's individual foliage elements (Ross, 1981), and it includes properties such as leaf area, leaf inclination (angle from zenith), leaf azimuth (angle from North in a clockwise direction) and leaf shape. Of these properties, the effect of leaf area and orientation (leaf inclination and azimuth) on solar radiation interception is most well understood. Their effect on solar radiation interception can also be mathematically described using Beer's law as shown by Monsi and Saeki (1953), and Ross (1981).

The effect of leaf shape, however, on solar radiation interception is little known. Its relationship with solar radiation interception is also not directly accounted for in Beer's law. All plant properties being equal, it is unclear how leaves having a given shape would *collectively* affect the solar radiation regime within the plant stand and thus the total solar radiation interception. Leaves with lobes, for example, are thought to reduce self-shading and to produce deeper sunflecks within a canopy (Horn, 1971). Computer simulations by Niklas (1989), however, revealed no change in the amount of daily solar radiation interception due to leaf lobbing *per se*. That the effect of leaf shape on solar radiation interception is unclear and little studied is not surprising. It is experimentally difficult to assess the effect of leaf shape on solar radiation interception because this factor cannot be isolated and studied independently from other plant or leaf factors (Niklas, 1989). It is impossible, for example, to find real plants that are identical in all aspects apart for their leaf shapes. One solution is to use computer-generated plants. By controlling all plant and leaf aspects, it is possible to study the effect of leaf shape *per se* on solar radiation interception.

It is thus the objective of this study to evaluate the effect of various leaf shapes on both direct and diffuse solar radiation interception using a detailed solar radiation model. If the role of leaf shape on solar radiation interception is shown to be important, this could help to better design or select crop varieties that have the "proper leaf form" for optimum plant production. This study would also help to understand the role of leaf shape as a plant adaptation mechanism to adapt to certain environmental conditions or stresses by altering, among others, the amount of solar radiation being captured.

2. Materials and methods

2.1. Model development

3-D solar radiation model

Beer's law can be used to determine the fraction or probability $P(r)$ of incident solar radiation coming from sun direction r that penetrates into the canopy:

$$P(r) = \exp[-k(r) \cdot L] \quad (1)$$

where L is the leaf area index, and $k(r)$ is the canopy extinction coefficient. Eq. (1), however, is too simplistic to asses the effect of leaf shape on solar radiation interception. This is because it is one-dimensional (*i.e.*, solar irradiance varies only in one direction); thus, it does not describe adequately how the spatial distribution of leaf area density is altered given a leaf shape. Consequently, it is essential to characterise both the canopy architecture and plant-radiation regime in the complete three dimensions.

The canopy space of a plant is divided into a network of 3-D cuboids that is perpendicular to the planting row direction (Fig. 1). The height, width and length of the network are equal to the plant height, inter-row and intra-row planting distance, respectively. In this study, the inter-row and intra-row planting distance were set at 0.6 and 0.3 m, respectively, and the planting row was in the North-South direction.

For each cuboid in the network, three kinds of information are required: a) leaf area density, b) leaf orientation distribution, or the G-function, and c) mean travelling distance of a solar beam. This information is required to calculate the probability $P_{dr,k}(r)$ of a single solar beam penetrating or exiting the k-th cuboid in the network:

$$P_{dr,k}(r) = \exp\left[-G_k(r) \cdot \rho_{f,k} \cdot s_k \cdot \sqrt{1-\sigma}\right] \cdot \prod_{c=1}^{k-1} \exp\left[-G_c(r) \cdot \rho_{f,c} \cdot s_c \cdot \sqrt{1-\sigma}\right] \quad (2)$$

where the multiplicative series c=1 to (k-1) represents every cuboid visited sequentially by the beam in reaching the target cuboid k; $G_c(r)$ is the G-function in the c-th cuboid; $\rho_{f,c}$ is the leaf area density in the c-th cuboid; s_c is the beam path length in the c-th cuboid; and σ is the leaf scatter coefficient, taken as 0.2 (Tournebize and Sinoquet, 1995). The so-called G-function $G(r)$ is regarded as the average projection per unit foliage area in the sun direction r, (Ross, 1981), where the sun direction r is described by solar inclination θ and azimuth ϕ. The $G_c(r)$ or $G_c(\theta, \phi)$ in the c-th cuboid is calculated by

$$G_c(\theta,\phi) = \sum_{j=1}^{N} L_{c,j} \left|\cos\theta\cos\theta_L + \sin\theta\sin\theta_L \cos(\phi - \phi_L)\right|_{c,j} \Big/ \sum_{j=1}^{N} L_{c,j} \quad (3)$$

where $L_{c,j}$ is area of the j-th leaf in the c-th cuboid; N is total number of leaves in c-th cuboid; and θ_L and ϕ_L are the leaf normal inclination and leaf normal azimuth of the j-th leaf in the c-th

cuboid, respectively. (Thanisawanyangkura *et al.*, 1997). Calculations for s_c are based on simple geometry as described by Gijzen and Goudriaan (1989), and Sinoquet and Bonhomme (1992).

In this study, a simulation run would begin by "pushing" a total of four equally-spaced beams (coming from solar direction *r*) into each cuboid in the uppermost level of the network. The traversal of each of these beams down the network was simulated using ray-tracing principles (Gijzen and Goudriaan, 1989; Sinoquet and Bonhomme, 1992). And for every cuboid that could be reached by a given beam direction, Eq. (2) was used to calculate the beam's penetration probability. This information is then stored. These steps were repeated for the traversal of the next beam "pushed" into the network. Consequently, at the end of a simulation run, the mean penetration probability for every cuboid in the network could be determined.

The total fraction of direct solar radiation intercepted F_{dr} is calculated by

$$F_{dr} = 1 - \overline{P_{dr,k=ground}(r)} \tag{4}$$

where $\overline{P_{dr,k=ground}(r)}$ is the average direct beam penetration probability for all cuboids on the ground level only (*i.e.*, the overall mean probability of a direct solar beam to reach the soil surface).

Unlike direct solar radiation, diffuse solar radiation does not come from a single direction but uniformly from all directions. The penetration probability of diffuse solar radiation $P_{df,k}$ in the *k*-th cuboid is approximated by summing the penetration probability of direct beams over the whole sky at three and four solar inclination θ and azimuth ϕ angles, respectively (θ = 15°, 30° and 75°, and ϕ = 45°, 135°, 225° and 315°), and taking the mean of the 12 values (de Castro and Fetcher, 1998), or

$$P_{df,k} = \frac{1}{12}\sum_{r} P_{dr,k}(r) = \frac{1}{12}\sum_{\theta}\sum_{\phi} P_{dr,k}(\theta,\phi) \tag{5}$$

The total fraction of diffuse solar radiation intercepted F_{df} is calculated by

$$F_{df} = 1 - \overline{P_{df,k=ground}} \tag{6}$$

where $\overline{P_{df,k=ground}}$ is the average diffuse beam penetration probability for all cuboids on the ground level only.

Finally, simulations of hourly solar radiation interception were done from 8:00 to 18:00 local hour, for the year 2003, day of year 152, and for site latitude and longitude of 3.24° N and 101.47° E, respectively.

3-D plant geometry

Located at the centre of the 3-D network of cuboids is a computer-generated plant (prototype) (Fig. 1) where, in this study, its leaf number, leaf azimuth, leaf position, planting distance, and plant height were held constant. Only its leaf shape, area and inclination were varied. Six simple shaped leaves were selected in this study to assess their effect on solar radiation interception: round (RD), square (SQ), triangle (TR), inverted triangle (ITR), ellipse (EL) and lobe (LB) (Fig. 2). The effect of these leaf shapes on solar radiation interception was examined in the following three conditions: a) leaf area index (LAI) 0.5, 1.0 and 3.0; b) leaf inclination 22.5°, 45° and 90°; and c) leaves with and without petioles.

In all of the above conditions, total plant height was set at 1.0 m, and the number of leaves per plant was set at 12 where the leaves were arranged in a whorled phyllotaxy with three leaves per node. Therefore every three leaves were positioned at four different plant heights (1.0, 0.7, 0.4 and 0.1 m), and for each height, the azimuth of the three leaves were separated from each other by 120°. The azimuths of the three leaves positioned at plant height 1.0 and 0.4 m were 0°, 120° and 240°, respectively, and the azimuths of three leaves positioned at plant height 0.7 and 0.1 m were 60°, 180° and 300°, respectively.

The area of every leaf in a plant was set equal to each other. Area per leaf was calculated by taking into account the leaf shape, number of leaves, planting distance and LAI. For example, given 12 leaves per plant, LAI 1.0 and planting distance of 0.6x0.3 m, the area and dimension (width by length) of every square leaf (SQ) per plant would be 0.0150 m^2 and 0.1225 by 0.1225 m, respectively. Note that the leaf shapes for prototypes SQ, TR and ITR were set as equilateral; that is, for a given shape, all its sides are equal (Fig. 2). For the EL prototype, the length of its elliptic leaf shape was set approximately double the leaf length of SQ prototype, and the widest leaf width for the EL occurred at half the leaf length. The length of the lobed leaves, LB, was set approximately equal to the leaf length of SQ prototype, and the length of the three equally-spaced lobes was set as half the total leaf length LB.

One of the properties required by Eq. (2) is the leaf area density within a cuboid. Because a leaf may not lie entirely within a cuboid, the leaves were described as 3-D polygons so that the Sutherland-Hodgman's 3-D polygon clipping algorithm (Sutherland and Hodgman, 1974) could be used to determine the section of a leaf polygon encompassed by a given cuboid. Applying this algorithm to all the leaves of the plant would give the total leaf area encompassed within

any cuboid. Leaf area density was calculated by dividing the enclosed leaf area by the cuboid volume.

2.2. Field experiment for model testing

To test the accuracy of the 3-D solar radiation model, model simulations were compared against actual measurements from a field experiment at various stages of crop growth. Maize (*Zea mays* L.) was planted in the North-South row direction at Research Field No. 2, Universiti Putra Malaysia (3.02° N, 101.70° E) on 5 June 2002. Field size was 18 by 18 m, with approximately six plants per m^2 ground area. Inter- and intra-row spacings were 0.6 and 0.3 m, respectively. Canopy architecture measurements on maize started 27 days after sowing (DAS) and continued every seven days for seven weeks. For each data collection period, three to six maize plants were randomly selected and all leaves in a plant were measured for their leaf azimuth, inclination, shape, curvature and area according to method by Stewart and Dwyer (1993) so that the leaves could be represented as 3-D polygons and used by the model. Solar irradiance above and below canopies were also measured diurnally during the data collection days, using a canopy transmission meter (Model EMS 7, Hitchin, Hertfordshire, UK) levelled horizontally and in perpendicular to the planting row direction.

3. Results and discussion

3.1. Model accuracy

It is not the purpose of this paper to discuss in detail the results obtained in the maize field experiment, but merely to establish confidence and accuracy of the 3-D model's simulations. Fig. 3 showed that the 3-D solar radiation model did not show any tendency to over- or underestimate the fraction of solar radiation captured by maize throughout its growing stages (from LAI 0.2 to 2.6). The model's mean absolute error MAE (average of the absolute differences between the simulated and measured values) was also low at 6.0%.

3.2. Effect of leaf shape on solar radiation interception

As expected, the mean hourly interception of solar radiation was effected by the leaf inclination and LAI (Table 1), where the interception of both direct and diffuse solar radiation increased with increasing LAI and leaf inclination (*i.e.*, increasingly larger and more horizontally inclined leaves).

Most importantly, however, given a leaf inclination and LAI, the mean hourly interception of solar radiation was effected by the leaf shape, albeit to a rather small extent (Table 1). The differences in solar radiation interception among the six plant prototypes were not more than

11% from each other. Moreover, their differences declined to not more than 5% from each other for full or near canopy cover (*i.e.*, LAI 3.0). At near or full canopy cover, the total fraction of direct or diffuse solar radiation intercepted was at near maximum 1.0; consequently, any further advantages of having a particular leaf shape to increase solar radiation interception at this stage would be small. As shown in Table 1, the mean hourly interception of both direct and diffuse solar radiation by the plant prototypes can be distinguished into two groups, where solar radiation interception decreased in the following manner: (ITR ≈ EL) > (RD ≈ SQ ≈ TR ≈ LB). Lobed leaves are often thought to alter the plant-radiation regime significantly by producing deeper sunflecks within the canopy (Horn, 1971). Nonetheless this study showed no effect of leaf lobbing *per se* (LB prototype) on solar radiation interception, as also reported by Niklas (1989). In his simulation study, the gaps between the leaf lobes of the short ragweed (*Ambrosia artemisiifolia* L.) were approximately 45% of the leaf area, and the gaps were numerous with each gap small and shallow. But in this study the gaps between the lobes for the LB prototype were approximately 30% of the leaf area, and these gaps were few with each gap wide and deep. Despite these differences in both these studies, leaf lobbing has so far been shown not to affect solar radiation interception.

The interception of both direct and diffuse solar radiation for all prototypes could however be further increased by the presence of leaf petioles (Table 2). Compared to sessile (non-petiole) leaves, leaves with petioles (100 mm in length) further increased the solar radiation interception by not more than 12%, but this increase generally declined for full or near canopy cover. Additionally, the interception of both direct and diffuse solar radiation by ITR and EL petiole leaves was at average 14% higher than that by RD sessile leaves. The increase in solar radiation interception due to the presence of petioles was generally most pronounced for RD, SQ, TR and LB plant prototypes (an average gain of 7%) as compared to ITR and EL prototypes (an average gain of 3%) (Table 2). This difference is because, as shown earlier, ITR and EL prototypes intercepted the most fraction of direct and diffuse solar radiation as compared to other plant prototypes. Thus, additional advantages of having leaf petioles to further increase solar radiation interception would be small for the EL and ITR prototypes.

Interestingly, stretching a leaf longer and narrower while maintaining the same leaf area augmented solar radiation interception (Fig. 4 and 5). The elliptic, sessile leaves for the EL prototype were stretched longer by 100 mm while maintaining the same leaf area. And compared to the non-modified EL leaves, the longer and narrower EL leaves further increased the interception of both direct and diffuse solar radiation by not more than 14%. This increase in interception, like the previous scenarios, declined for full or near canopy cover.

For every prototype, there was a strong negative correlation coefficient between the mean solar radiation intercepted and the coefficient of variation (c.v.) of leaf area density (Fig. 6). Because all plant properties were held constant in this study, a low c.v. value of leaf area density would indicate a more uniform spread or distribution of leaf area in the canopy aerial space. This in turn means lesser self-shading and clumping of leaves. Fig. 7a shows that, for all plant prototypes, the c.v. values of leaf area density for petiole leaves were lower than that for sessile leaves. This corresponded to the earlier observation that prototypes with petiole leaves intercepted more solar radiation than that by prototypes with sessile leaves. Also observed earlier was that the EL modified leaves (leaves modified to be longer and narrower) intercepted more solar radiation that that by the EL non-modified leaves. This again was consistent to the lower c.v. values for EL modified leaves as compared to the c.v. values for EL non-modified leaves (Fig. 7b). This study also showed that although TR and ITR prototypes had both triangle leaves, ITR intercepted more solar radiation than TR because the orientation of ITR leaves was such that the bulk of the leaf area was away from the plant stem (*i.e.*, leaves broader at their apex than at their basal) which reduced clustering of leaves around the plant stem which in turn lowered the c.v. of leaf area density.

The degree of leaf clustering was also evident when a modified version of Eq. (1) was applied. Beer's law assumes a random and homogenous distribution of leaves, but leaves in nature have finite dimensions and are rarely arranged in perfect randomness. To correct for this violation, a leaf clustering coefficient Ω is typically introduced into Eq. (1):

$$P(r) = \exp\left[-k(r)\cdot\Omega\cdot L\right] \tag{7}$$

where Ω ranges from 0 (strong violation; much leaf clustering) to 1 (no violation; random leaf arrangement) (Goudriaan and van Laar, 1994). Table 3 shows the mean hourly Ω values for the various prototypes, where the mean Ω value for a given prototype was obtained by minimizing the differences between the hourly simulation results from the 3-D solar radiation model and the simpler Eq. (7). Table 3 supports the c.v. results previously obtained, where the RD, SQ, TR and LB prototypes had similar but smaller Ω values than that for the ITR and EL prototypes.

Results presented here indicated that leaf shape does have an effect on solar radiation interception (though to a rather small extent) by altering the spatial distribution of leaf area density. Solar radiation interception is augmented for plants having leaves that are shaped in such a way that causes the canopy to be "spread out" more uniformly or homogenously; thus, reducing self-shading or clustering of leaves. Plants with long, narrow leaves, for example, increases solar radiation interception as compared to plants with short, wide leaves. This indicate that, all properties being equal, grass species, maize and oil palm trees, due to their

long, narrow leaves, would intercept more solar radiation than plants that have short, wide leaves. Leaves that are broader at the apex than at the basal would also increase solar radiation interception because this reduces the bunching or clustering of leaves near the plant stem, causing a more uniform spread of leaf area. This would mean that, all properties being equal, plants having leaf shapes that are broad at the apex such as oblanceolate, obovate and spatulate (Glattstein, 2003) would intercept more solar radiation than plants having leaf shapes that are broad at the basal such as ovate and cordate. Leaf petioles also increase solar radiation interception in particular by reducing leaf clustering around the plant stem, but the advantages of having leaf petioles are least pronounced for plants that have long, narrow leaves. This may indicate why plants having such leaves rarely have petioles (*e.g.*, maize and oil palm) as they already capture solar radiation effectively.

The results here may indicate that crop yields could be increased, albeit slightly, by designing or selecting crop varieties that have longer and narrower leaves, leaves with longer petioles, or leaves that are broader at their apex than at their basal. Nonetheless, in stressed environments, having such leaves may be detrimental due to the heavy solar radiation load on them. In such conditions, short and wide sessile leaves may instead be more preferable. Bailey and Sinnott (1916) reported that environment factors have a stronger effect on leaf form and size than the plants' genetic make-up. This highlights the importance of plant adaptation mechanisms in certain environment conditions or stresses. For a given leaf area, narrow leaves are found to have lower evaporation rates as compared to broad leaves (Taylor, 1975) due to the thicker boundary layer of non-moving air on the narrow leaves. Leaf rolling and drooping are also mechanisms to reduce thermal load and evaporation losses (Campbell and Norman, 2000). Results from this study and from Niklas (1989) indicate that the function of leaf lobes is probably more associated to the adaptation to heat and water loss rather than to adaptation to solar radiation interception. Leaves with lobes are found to convectively dissipate heat most easily as compared to other leaf shapes as found by Vogel (1970), which are advantageous in hot, dry environments.

Finally, the differences in leaf shapes did not appear to affect the diurnal variation of direct solar radiation interception (Fig. 8), where for each plant prototype, the interception of direct solar radiation depended on the solar position, whereby the solar radiation interception decreased gradually as the sun begun to align in parallel to the planting row direction (N-S) at 13:00 hours at this site. Direct solar radiation interception decreased and was at the lowest at 13:00 hours, and after this hour solar radiation interception gradually increased. The effect of a pronounced planting row direction on solar radiation capture has often been observed (Wallace 1997). This effect arises because when the sun is parallel to the planting row direction the

impediment by the canopies on solar beams is less as compared to that when the sun is non-parallel to the planting row direction. With increasing leaf inclination, the diurnal variation of direct solar radiation interception would decrease; that is, becoming more constant throughout the day. It is widely known that the interception of solar radiation by horizontal leaves is not effected by the solar position (Goudriaan and van Laar, 1994). Unlike the diurnal variation in direct solar radiation interception, the diffuse solar radiation interception was constant throughout the day (no diurnal variation) (Fig. 9) because diffuse solar radiation was considered in this study to radiate uniformly from all directions of the whole sky; thus, the canopy architecture and solar position have no effect on the diurnal variation of the fraction of diffuse solar radiation intercepted (*see also* Fig. 5).

4. Conclusion

Leaf shape was shown to have an effect on solar radiation interception, although its effect was to a rather small degree of not more than 11% increase in solar radiation interception. All plant properties being equal, solar radiation interception could be increased by having leaf shapes that are: 1) long and narrow, 2) broader at the apex than at the basal, and 3) supported by leaf petioles. These three conditions increase solar radiation interception by reducing leaf clustering and self-shading especially near the plant stem. In short, leaf shapes that increase solar radiation interception are those that cause the canopy to be spread out more uniformly or homogenously in the aerial space.

References

Bailey, I.W., Sinnott, E.W. 1916. The climatic distribution of certain types of angiosperm leaves. Am. J. Bot. 3, 24-39.

Campbell, G.S., Norman, J.M. 1998. An Introduction to Environmental Biophysics. 2nd. edn. Springer-Verlag, New York.

de Castro, F., Fetcher, N. 1998. Three dimensional model of the interception of light by a canopy. Agric. For. Meteorol. 90, 215-233.

Gijzen, H., Goudriaan, J. 1989. A flexible and explanatory model of light distribution and photosynthesis in row crops. Agric. For. Meteorol. 48, 1-20.

Glattstein, J. 2003. Consider the Leaf: Foliage in Garden Design. Timber Press, Portland, Oregon.

Goudriaan, J., van Laar, H.H. 1994. Modelling Potential Crop Growth Processes. A Textbook with Exercise. Current Issues in Production Ecology. Vol 2. Kluwer Academic, Netherlands.

Horn, H.S. 1971. The Adaptive Geometry of Trees. Princeton University Press, Princeton NJ.

Monsi, M., Saeki, T. 1953. Über den lichtfactor in den pflanzengesellschaften und seine bedeutung fur die stoffproduktion. Jap. J. Bot., 14, 22-52.

Niklas, K.J. 1989. The effect of leaf-lobbing on the interception of direct solar radiation. Oecologia. 80, 59-64.

Ross, J. 1981. The Radiation Regime and Architecture of Plant Stands. W. Junk, The Hague.

Sinoquet, H., Bonhomme, R. 1992. Modelling radiative transfer in mixed and row intercropping systems. Agric. For. Meteorol. 62, 219-240.

Stewart, D.W., Dwyer, L.M. 1993. Mathematical characterization of maize canopies. Agric. For. Meteorol. 66, 247-265.

Sutherland, I.E., Hodgman, G.W. 1974. Reentrant polygon clipping. CACM, 17, 32-42

Taylor, S.E. 1975. Optimal leaf form. Perspectives in Biophysical Ecology. In: Gates, D.M., Schmerl, R.B. (Eds.) Springer-Verlag, New York, pp. 73-86.

Thanisawanyangkura, S., Sinoquet, H., Rivet, P., Cretenet, M., Jallas, E. 1997. Leaf orientation and sunlit leaf area distribution in cotton. Agric. For. Meteorol. 86, 1-15.

Tournebize, R. Sinoquet, H. 1995. Light interception and partitioning in a shrub/grass mixture. Agric. For. Meteorol. 72, 277-294.

Vogel, S. 1970. Convective cooling at low airspeeds and the shapes of broad leaves. J. Exp. Bot. 21, 91-101.

Wallace, J.S. 1997. Evaporation and radiation interception by neighbouring plants. Quarterly J. Royal Meteorol. Soc. 123, 1885-1905.

Table 1

Mean hourly fraction of intercepted solar radiation for all plant prototypes with sessile (non-petiole) leaves. Note: in the same table column, values in the brackets indicate the difference (in percent) from the fraction of solar radiation intercepted by the RD prototype.

(a) Direct solar radiation

Proto-	**LAI 0.5**				**LAI 1**				**LAI 3**			
type	**22.5°**	**45°**	**90°**	**Mean**	**22.5°**	**45°**	**90°**	**Mean**	**22.5°**	**45°**	**90°**	**Mean**
RD	0.258	0.278	0.279	0.272	0.401	0.458	0.472	0.443	0.722	0.812	0.848	0.794
	(0.0)	*(0.0)*	*(0.0)*	*(0.0)*	*(0.0)*	*(0.0)*	*(0.0)*	*(0.0)*	*(0.0)*	*(0.0)*	*(0.0)*	*(0.0)*
SQ	0.267	0.283	0.281	0.277	0.407	0.464	0.473	0.448	0.729	0.816	0.849	0.798
	(3.4)	*(1.9)*	*(0.8)*	*(2.0)*	*(1.6)*	*(1.3)*	*(0.1)*	*(0.9)*	*(0.9)*	*(0.4)*	*(0.1)*	*(0.5)*
TR	0.261	0.280	0.275	0.272	0.415	0.462	0.469	0.449	0.731	0.812	0.842	0.795
	(1.1)	*(0.9)*	*(-1.1)*	*(0.3)*	*(3.6)*	*(1.0)*	*(-0.7)*	*(1.2)*	*(1.3)*	*(0.0)*	*(-0.6)*	*(0.2)*
ITR	0.279	0.306	0.299	0.295	0.440	0.498	0.505	0.481	0.751	0.839	0.876	0.822
	(8.2)	*(10.2)*	*(7.4)*	*(8.6)*	*(9.8)*	*(8.8)*	*(7.0)*	*(8.5)*	*(4.0)*	*(3.3)*	*(3.3)*	*(3.5)*
EL	0.275	0.307	0.305	0.295	0.442	0.496	0.508	0.482	0.750	0.833	0.878	0.820
	(6.3)	*(10.6)*	*(9.3)*	*(8.6)*	*(10.2)*	*(8.4)*	*(7.7)*	*(8.7)*	*(3.9)*	*(2.6)*	*(3.6)*	*(3.3)*
LB	0.264	0.280	0.258	0.267	0.417	0.462	0.456	0.445	0.734	0.812	0.839	0.795
	(2.3)	*(0.8)*	*(-7.4)*	*(-1.5)*	*(4.2)*	*(1.0)*	*(-3.5)*	*(0.4)*	*(1.7)*	*(0.0)*	*(-1.1)*	*(0.1)*

(b) Diffuse solar radiation

Proto-	**LAI 0.5**				**LAI 1**				**LAI 3**			
type	**22.5°**	**45°**	**90°**	**Mean**	**22.5°**	**45°**	**90°**	**Mean**	**22.5°**	**45°**	**90°**	**Mean**
RD	0.283	0.293	0.303	0.293	0.438	0.482	0.509	0.476	0.726	0.813	0.874	0.804
	(0.0)	*(0.0)*	*(0.0)*	*(0.0)*	*(0.0)*	*(0.0)*	*(0.0)*	*(0.0)*	*(0.0)*	*(0.0)*	*(0.0)*	*(0.0)*
SQ	0.291	0.300	0.305	0.299	0.445	0.486	0.511	0.481	0.700	0.814	0.874	0.796
	(3.0)	*(2.5)*	*(0.8)*	*(2.1)*	*(1.7)*	*(0.8)*	*(0.3)*	*(0.9)*	*(-3.7)*	*(0.1)*	*(0.0)*	*(-1.1)*
TR	0.295	0.300	0.298	0.298	0.463	0.491	0.509	0.487	0.739	0.810	0.867	0.805
	(4.5)	*(2.5)*	*(-1.6)*	*(1.7)*	*(5.7)*	*(1.8)*	*(-0.1)*	*(2.3)*	*(1.8)*	*(-0.4)*	*(-0.8)*	*(0.1)*
ITR	0.295	0.324	0.326	0.315	0.472	0.521	0.538	0.510	0.758	0.845	0.907	0.837
	(4.5)	*(10.6)*	*(7.7)*	*(7.6)*	*(7.9)*	*(8.1)*	*(5.7)*	*(7.2)*	*(4.3)*	*(4.0)*	*(3.8)*	*(4.0)*
EL	0.303	0.325	0.331	0.319	0.476	0.520	0.546	0.514	0.753	0.851	0.908	0.838
	(7.3)	*(10.8)*	*(9.1)*	*(9.1)*	*(8.8)*	*(7.8)*	*(7.3)*	*(7.9)*	*(3.7)*	*(4.7)*	*(4.0)*	*(4.2)*
LB	0.294	0.301	0.280	0.292	0.462	0.491	0.493	0.482	0.742	0.813	0.863	0.806
	(4.1)	*(2.9)*	*(-7.5)*	*(-0.3)*	*(5.5)*	*(1.8)*	*(-3.2)*	*(1.2)*	*(2.1)*	*(0.0)*	*(-1.2)*	*(0.2)*

Table 2

Mean hourly fraction of intercepted solar radiation for all plant prototypes with petiole leaves. Note: the values in the brackets indicate the difference (in percent) between the fraction of solar radiation intercepted by sessile (non-petiole) and petiole leaves of the same prototype, LAI and leaf inclination (*i.e*, compare with Table 1).

(a) Direct solar radiation

Proto-	**LAI 0.5**				**LAI 1**				**LAI 3**			
type	**22.5°**	**45°**	**90°**	**Mean**	**22.5°**	**45°**	**90°**	**Mean**	**22.5°**	**45°**	**90°**	**Mean**
RD	0.283	0.302	0.291	0.292	0.438	0.488	0.488	0.472	0.743	0.826	0.874	0.815
	(9.6)	*(8.6)*	*(4.5)*	*(7.5)*	*(9.4)*	*(6.5)*	*(3.5)*	*(6.3)*	*(2.9)*	*(1.8)*	*(3.1)*	*(2.6)*
SQ	0.287	0.309	0.302	0.299	0.446	0.499	0.501	0.482	0.749	0.839	0.882	0.823
	(7.2)	*(9.3)*	*(7.5)*	*(8.0)*	*(9.5)*	*(7.7)*	*(6.1)*	*(7.7)*	*(2.7)*	*(2.8)*	*(3.9)*	*(3.2)*
TR	0.287	0.311	0.306	0.301	0.453	0.502	0.507	0.488	0.753	0.838	0.881	0.824
	(9.7)	*(11.0)*	*(11.0)*	*(10.6)*	*(9.2)*	*(8.7)*	*(8.2)*	*(8.7)*	*(3.0)*	*(3.3)*	*(4.6)*	*(3.6)*
ITR	0.299	0.314	0.303	0.306	0.458	0.495	0.513	0.489	0.766	0.849	0.885	0.833
	(7.1)	*(2.8)*	*(1.3)*	*(3.7)*	*(4.2)*	*(-0.5)*	*(1.5)*	*(1.6)*	*(2.1)*	*(1.1)*	*(1.0)*	*(1.4)*
EL	0.295	0.316	0.316	0.309	0.460	0.505	0.524	0.496	0.764	0.835	0.872	0.824
	(7.4)	*(2.9)*	*(3.8)*	*(4.6)*	*(4.2)*	*(1.8)*	*(3.0)*	*(3.0)*	*(1.9)*	*(0.2)*	*(-0.7)*	*(0.4)*
LB	0.289	0.312	0.284	0.295	0.456	0.502	0.482	0.480	0.750	0.838	0.872	0.820
	(9.2)	*(11.3)*	*(9.9)*	*(10.1)*	*(9.2)*	*(8.6)*	*(5.8)*	*(7.8)*	*(2.2)*	*(3.3)*	*(4.0)*	*(3.2)*

(b) Diffuse solar radiation

Proto-	**LAI 0.5**				**LAI 1**				**LAI 3**			
type	**22.5°**	**45°**	**90°**	**Mean**	**22.5°**	**45°**	**90°**	**Mean**	**22.5°**	**45°**	**90°**	**Mean**
RD	0.315	0.319	0.318	0.317	0.477	0.512	0.531	0.507	0.750	0.842	0.905	0.832
	(11.5)	*(8.8)*	*(4.8)*	*(8.3)*	*(9.0)*	*(6.1)*	*(4.2)*	*(6.3)*	*(3.3)*	*(3.6)*	*(3.6)*	*(3.5)*
SQ	0.321	0.328	0.329	0.326	0.485	0.524	0.542	0.517	0.755	0.849	0.913	0.839
	(10.2)	*(9.4)*	*(7.6)*	*(9.1)*	*(9.0)*	*(7.7)*	*(6.2)*	*(7.6)*	*(7.9)*	*(4.4)*	*(4.4)*	*(5.4)*
TR	0.322	0.332	0.331	0.328	0.492	0.530	0.547	0.523	0.755	0.847	0.910	0.837
	(9.0)	*(10.8)*	*(10.9)*	*(10.2)*	*(6.3)*	*(8.0)*	*(7.5)*	*(7.3)*	*(2.0)*	*(4.6)*	*(5.0)*	*(4.0)*
ITR	0.325	0.331	0.334	0.330	0.492	0.527	0.552	0.524	0.768	0.865	0.913	0.849
	(10.3)	*(2.1)*	*(2.5)*	*(4.8)*	*(4.2)*	*(1.2)*	*(2.6)*	*(2.6)*	*(1.4)*	*(2.3)*	*(0.7)*	*(1.5)*
EL	0.322	0.335	0.343	0.333	0.492	0.534	0.563	0.530	0.776	0.866	0.902	0.848
	(6.1)	*(3.3)*	*(3.8)*	*(4.4)*	*(3.4)*	*(2.6)*	*(3.0)*	*(3.0)*	*(3.0)*	*(1.7)*	*(-0.7)*	*(1.2)*
LB	0.323	0.333	0.305	0.321	0.495	0.530	0.519	0.515	0.755	0.847	0.903	0.835
	(10.0)	*(10.6)*	*(9.0)*	*(9.9)*	*(7.1)*	*(8.0)*	*(5.3)*	*(6.8)*	*(1.7)*	*(4.2)*	*(4.7)*	*(3.6)*

Table 3

Leaf clustering coefficient (Ω) for plant prototypes having sessile and petiole leaves

Prototype	Solar radiation component	Ω	
		Sessile	Petiole
RD	Direct	0.74	0.81
	Diffuse	0.77	0.84
SQ	Direct	0.75	0.85
	Diffuse	0.77	0.86
TR	Direct	0.74	0.86
	Diffuse	0.78	0.88
ITR	Direct	0.83	0.86
	Diffuse	0.82	0.89
EL	Direct	0.82	0.90
	Diffuse	0.82	0.90
LB	Direct	0.77	0.84
	Diffuse	0.76	0.84

Fig. 1. The canopy aerial space is divided into a network of 3-D cuboids, where the computer-generated plant is located at the centre of the network

Fig. 2. Leaf shapes for the six plant prototypes: round (RD), square (SQ), triangle (TR), inverted triangle (ITR), ellipse (EL) and lobe (LB)

Fig. 3. Comparisons between the simulated and measured total fraction of intercepted solar radiation by the maize crop

Fig. 4. Comparisons between the fraction of intercepted direct solar radiation by the EL (modified) and EL (normal) prototypes. Note: values in brackets indicate the mean hourly difference (in percent) between the fraction of intercepted solar radiation by the EL (modified) and EL (normal) prototypes.

Fig. 5. Comparisons between the fraction of intercepted diffuse solar radiation by the EL (modified) and normal EL prototypes. Note: values in brackets indicate the mean hourly difference (in percent) between the fraction of intercepted solar radiation by the EL (modified) and EL (normal) prototypes.

Fig. 6. Relationship between the coefficient of variation of leaf area density (CV) and the fraction of intercepted direct (DR) and diffuse (DF) solar radiation for all the plant prototypes

Fig. 7. Relationship between the coefficient of variation (c.v.) of leaf area density for: (a) all plant prototypes having petiole and sessile leaves, and (b) EL (modified) and normal EL prototypes

Fig. 8. Diurnal fraction of intercepted direct solar radiation for the EL, LB and RD plant prototypes. Note: other plant prototypes showed similar diurnal variation.

Fig. 9. Diurnal fraction of intercepted diffuse solar radiation for the EL, LB and RD plant prototypes. Note: other plant prototypes showed similar diurnal variation.

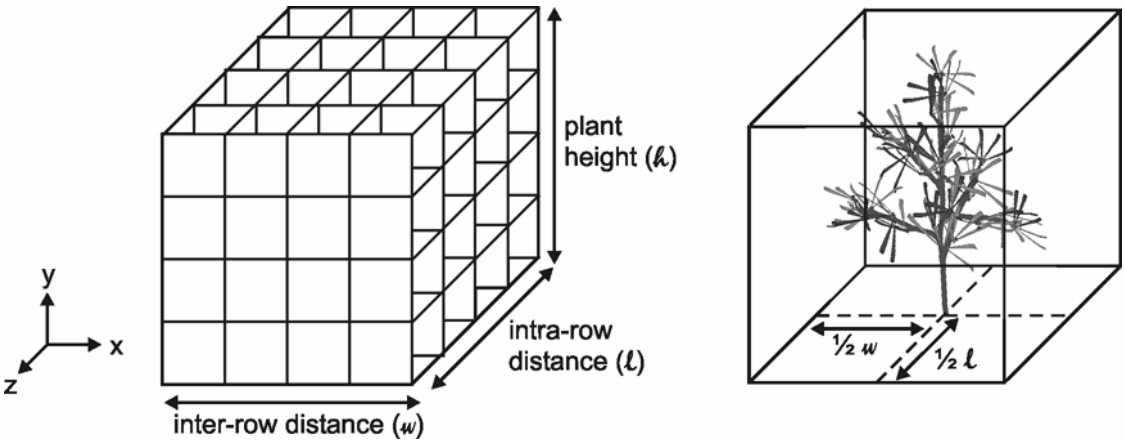
plant
height (h)
y
x
z
intra-row
distance (l)
inter-row distance (w)
½ w
½ l

Fig. 1

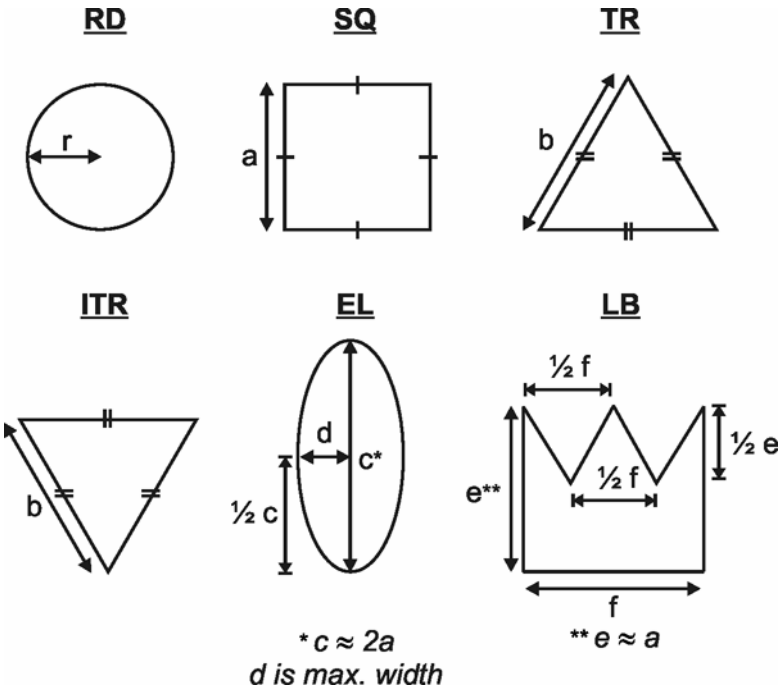

Fig. 2

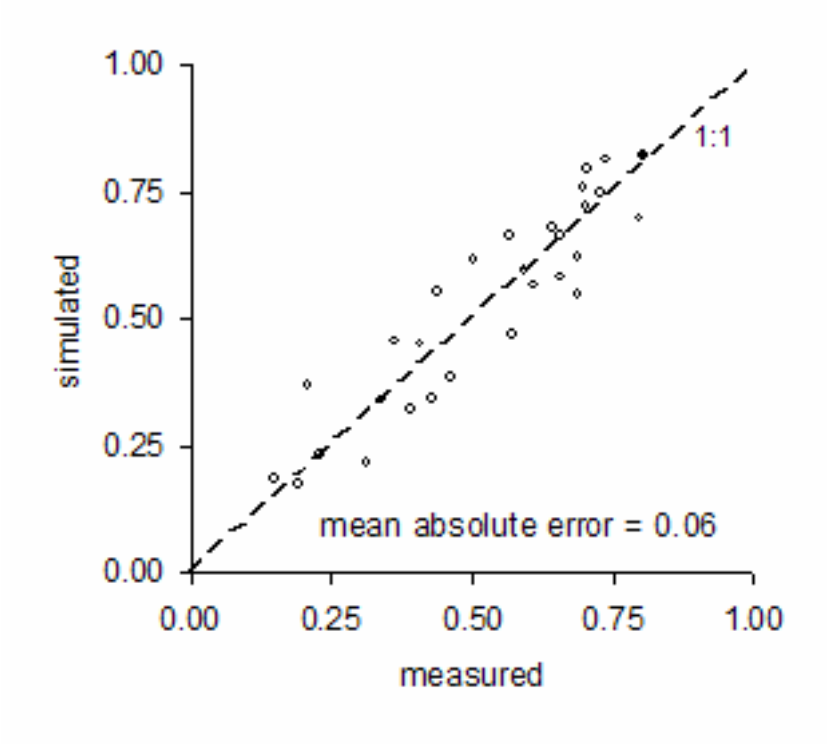
1.00
0.75
0.50
0.25
0.00
simulated
1:1
mean absolute error = 0.06
0.00
0.25
0.50
0.75
1.00
measured

Fig. 3

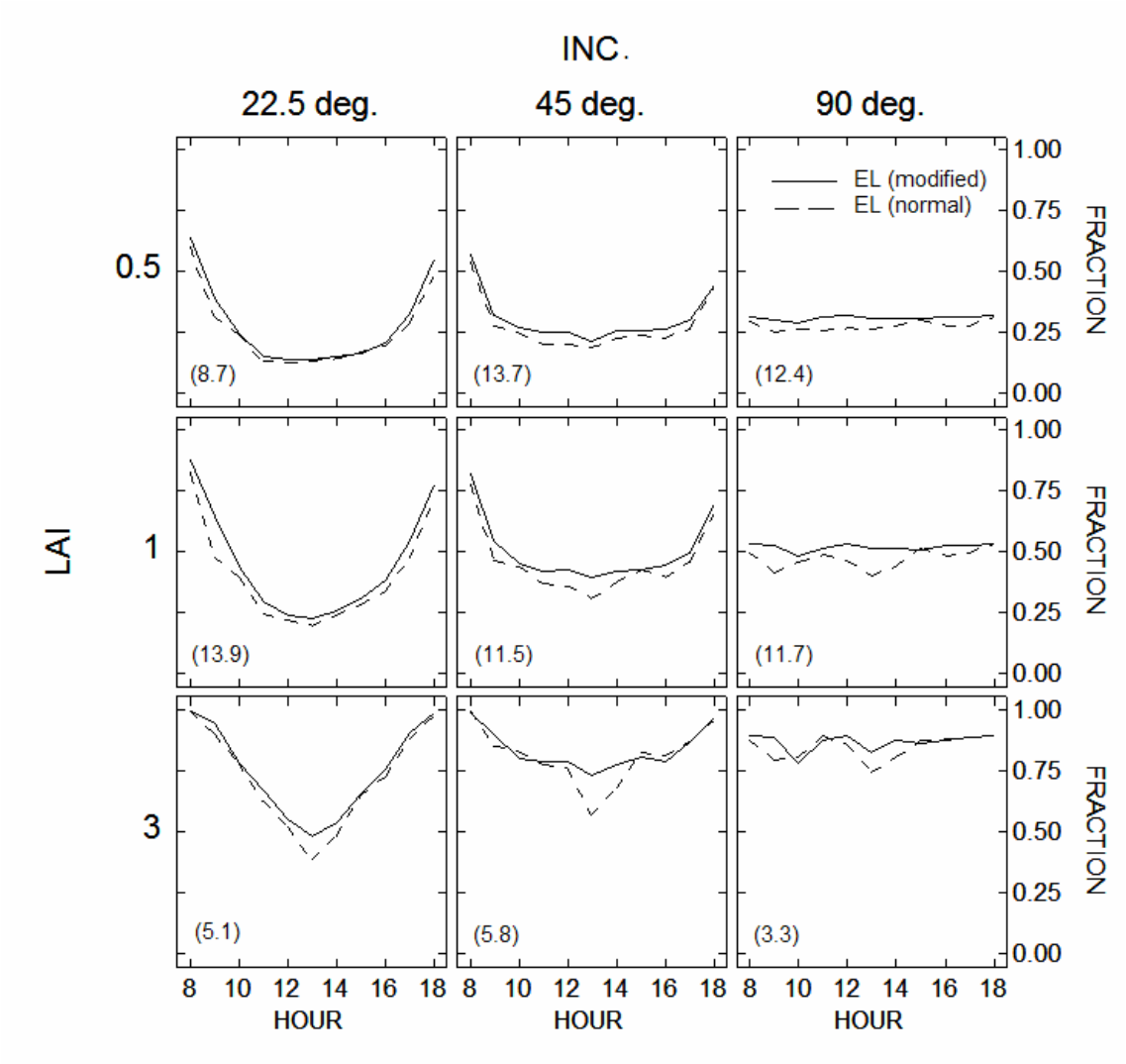
INC.
22.5 deg.
45 deg.
90 deg.
LAI
0.5
1
3
EL (modified)
EL (normal)
(8.7)
(13.7)
(12.4)
(13.9)
(11.5)
(11.7)
(5.1)
(5.8)
(3.3)
FRACTION
1.00
0.75
0.50
0.25
0.00
8 10 12 14 16 18
HOUR

Fig. 4

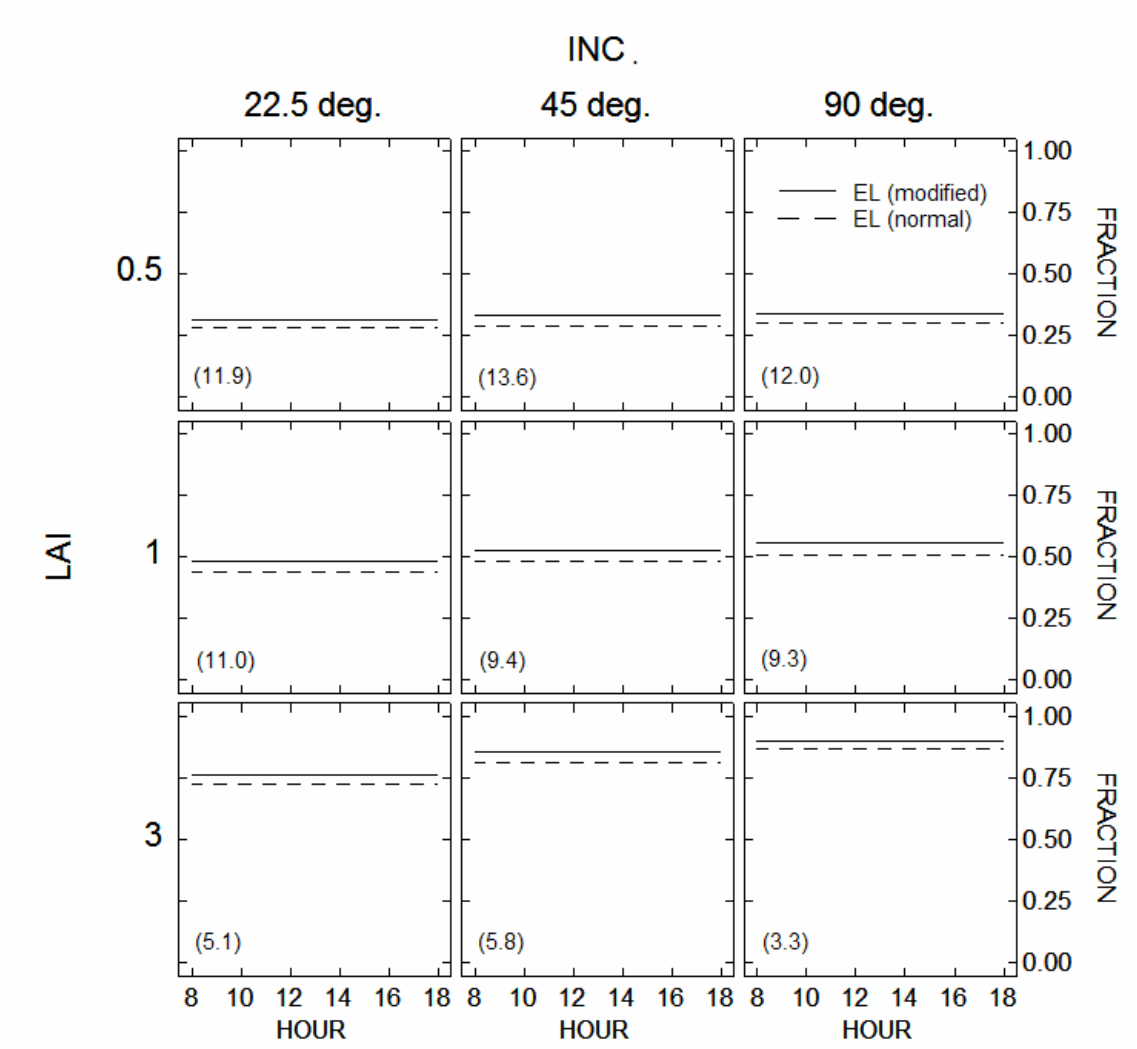
INC.
22.5 deg.
45 deg.
90 deg.
LAI
0.5
1
3
EL (modified)
EL (normal)
(11.9)
(13.6)
(12.0)
(11.0)
(9.4)
(9.3)
(5.1)
(5.8)
(3.3)
FRACTION
1.00
0.75
0.50
0.25
0.00
8 10 12 14 16 18
HOUR

Fig. 5

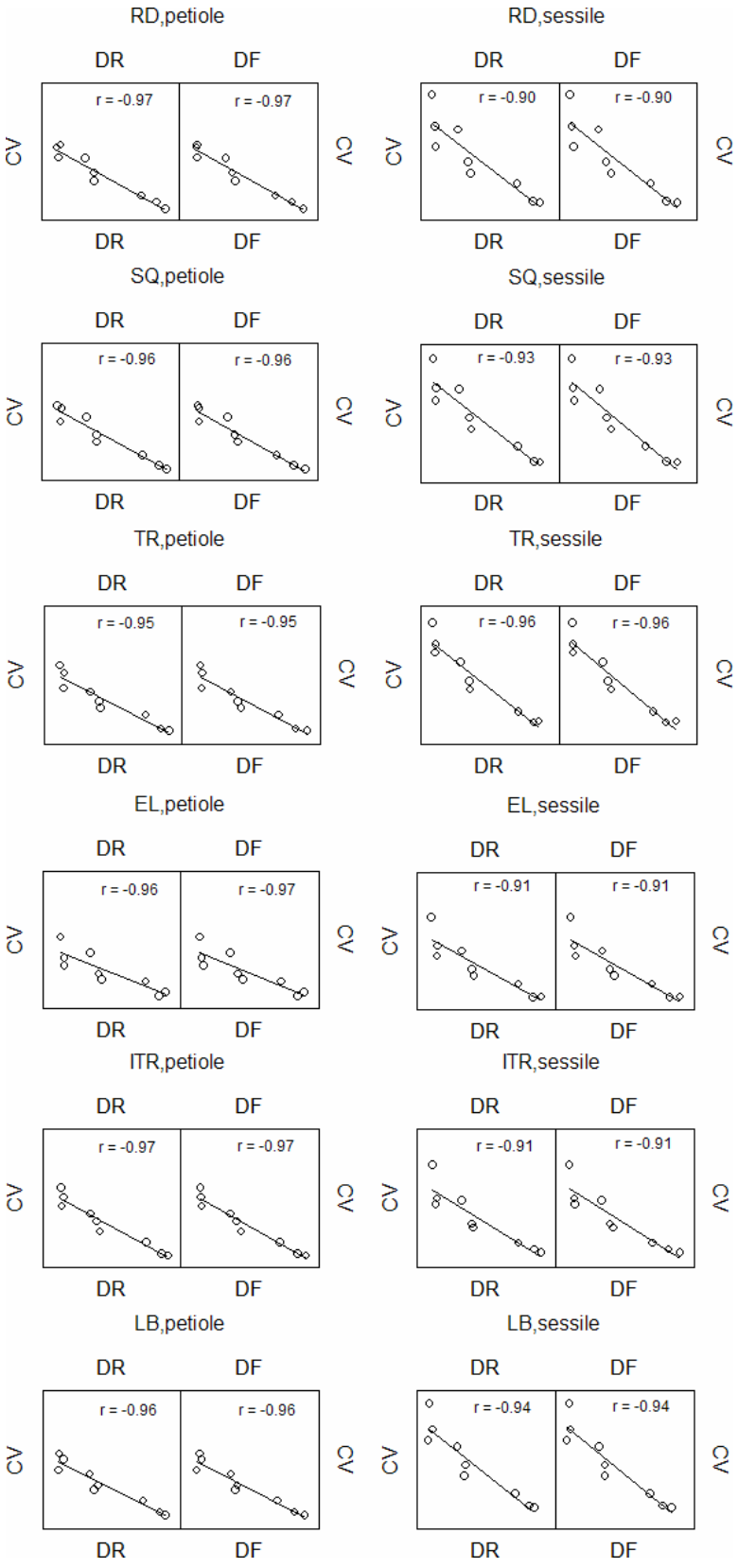
RD,petiole
DR
DF
r = -0.97
r = -0.97
CV
CV
DR
DF
RD,sessile
DR
DF
r = -0.90
r = -0.90
CV
CV
DR
DF
SQ,petiole
DR
DF
r = -0.96
r = -0.96
CV
CV
DR
DF
SQ,sessile
DR
DF
r = -0.93
r = -0.93
CV
CV
DR
DF
TR,petiole
DR
DF
r = -0.95
r = -0.95
CV
CV
DR
DF
TR,sessile
DR
DF
r = -0.96
r = -0.96
CV
CV
DR
DF
EL,petiole
DR
DF
r = -0.96
r = -0.97
CV
CV
DR
DF
EL,sessile
DR
DF
r = -0.91
r = -0.91
CV
CV
DR
DF
ITR,petiole
DR
DF
r = -0.97
r = -0.97
CV
CV
DR
DF
ITR,sessile
DR
DF
r = -0.91
r = -0.91
CV
CV
DR
DF
LB,petiole
DR
DF
r = -0.96
r = -0.96
CV
CV
DR
DF
LB,sessile
DR
DF
r = -0.94
r = -0.94
CV
CV
DR
DF

Fig. 6

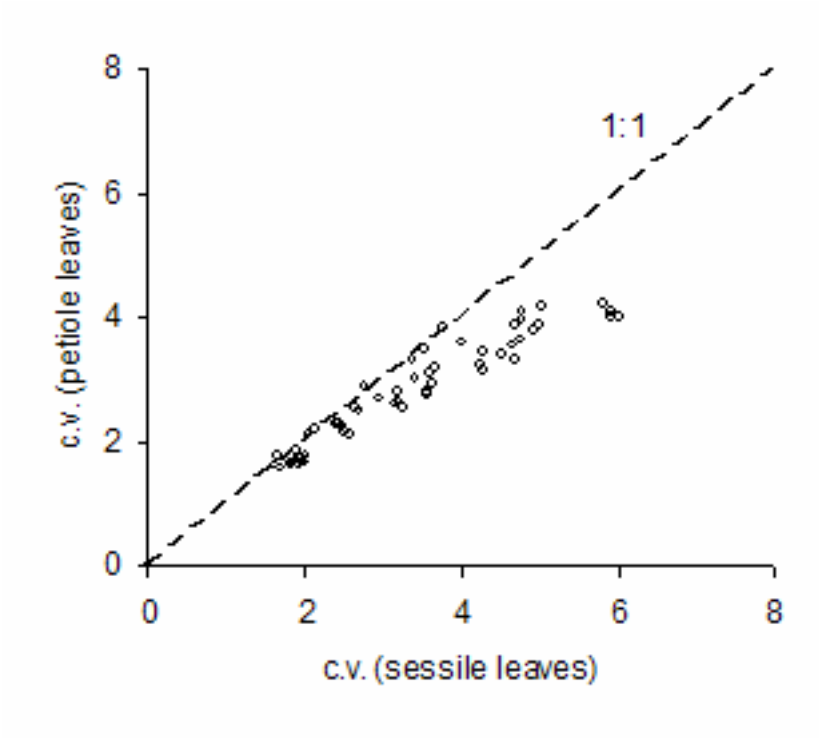
1:1
c.v. (petiole leaves)
c.v. (sessile leaves)
0
2
4
6
8

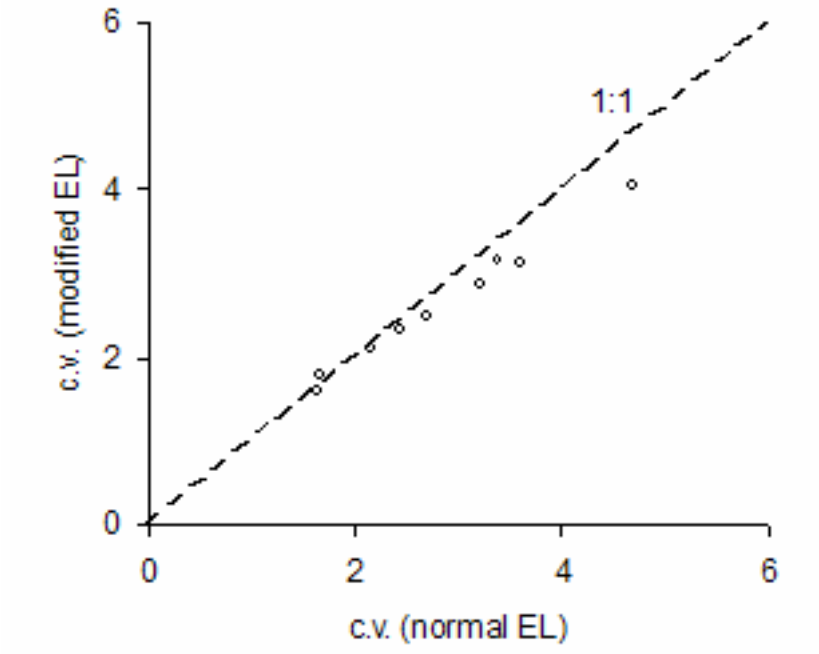
1:1
c.v. (modified EL)
c.v. (normal EL)
0
2
4
6

Fig. 7 a & b

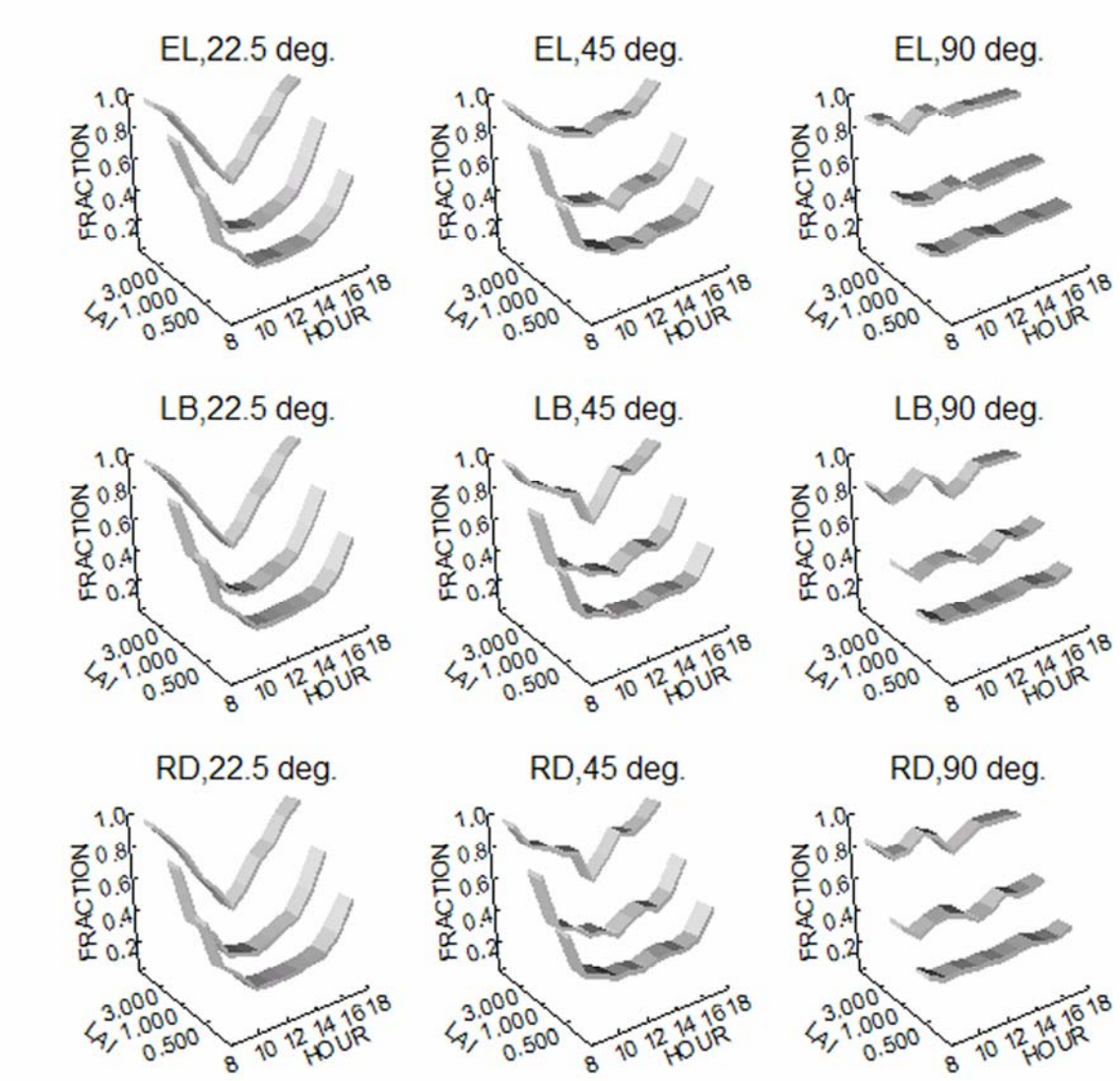
EL,22.5 deg.
EL,45 deg.
EL,90 deg.
LB,22.5 deg.
LB,45 deg.
LB,90 deg.
RD,22.5 deg.
RD,45 deg.
RD,90 deg.
FRACTION
1.0
0.8
0.6
0.4
0.2
LA/
3.000
1.000
0.500
8
10 12 14 16 18
HOUR

Fig. 8

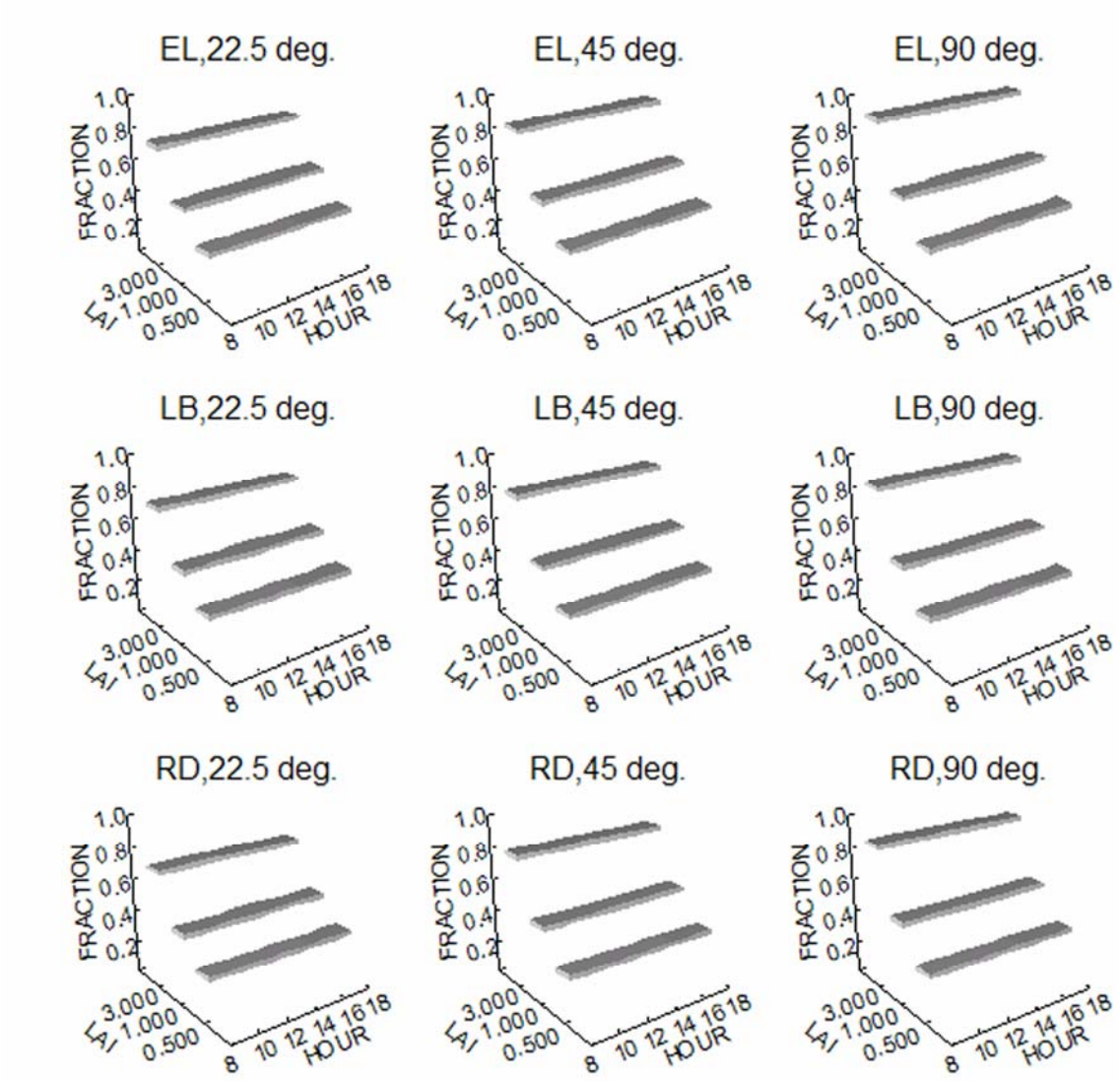
EL,22.5 deg.
EL,45 deg.
EL,90 deg.
LB,22.5 deg.
LB,45 deg.
LB,90 deg.
RD,22.5 deg.
RD,45 deg.
RD,90 deg.
FRACTION
1.0
0.8
0.6
0.4
0.2
LA
3.000
1.000
0.500
8
10 12 14 16 18
HOUR

Fig. 9